# Comparison of FDDO and DSMC Methods in the Analysis of Expanding Rarefied Flows

C. H. Chung*1

## 팽창희박류의 분석에 있어서 FDDO와 직접모사법의 비교

정 찬 홍

이차원 노즐을 통하여 저밀도 환경으로 팽창하는 희박류의 분석에 있어서 불연속좌표법과 결합된 유한차분법(finite-difference method coupled with the discrete-ordinate method, FDDO)과 직접모사법(direct-simulation Monte-Carlo method, DSMC)이 비교되었다. FDDO를 이용한 분석에서는 충돌적분모델을 도입하여 간단해진 볼츠만식(Boltzmann equation)이 불연속좌표법을 이용하여 물리적 공간에서는 연속이나 분자속도 공간에서는 불연속좌표로 표시되는 편미분방정식군으로 변환되어 유한차분법에의하여 수치해석 되었다. 직접모사법에서는 분자모델로 가변강구모델(variable hard sphere model, VHS)이, 충돌샘플링모델로는 비시계수법(no time counter method, NTC)이 채택되었다. 전혀 다른 두 가지 방법에 의한 노즐 내부에서의 유체흐름 해석결과는 매우 잘 일치하였으며, 노즐 외부의 plume 영역에서는 FDDO에 의한 해석결과가 직접모사법에 의한 해석결과에 비하여 약간 느린 팽창을 보였다.

**Key Words:** 희박기체흐름(Rarefied Gas Flow), 노즐흐름(Nozzle Flow), 불연속좌표법(Discrete-Ordinat Method), 유한차분법(Finite-Difference Method), 직접모사법(DSMC)

## 1. Introduction

The flow of a gas expanding through a nozzle and into a surrounding low-density environment is one of the important problems in the field of gas dynamics. Applications of this type of flow are found in vacuum science and high altitude flight such as the flow field for low-thrust resistojets. This type of flow involves high angled backflow, in which strong nonequilibrium effects due to rapid expansion into a low-density environment play an important role. The fluid experiences continuum, transition, and free-molecular flow regimes. Consequently, the conventional continuum gas dynamics may not be adequate and an approach based on molecular gas dynamics is required for the analysis of the flow.

The direct simulation Monte-Carlo(DSMC) method [1] is a simulation technique for the computer modeling of a real gas flow by a representative set of molecules. The movements and collisions between the molecules are decoupled for a discrete time interval.

*1 정회원, 대구대학교 화학공학과

The velocity and position of the set of molecules during the discrete time interval are modified as the molecules are concurrently followed through collisions and boundary interactions in simulated physical space.

The finite-difference method coupled with the discrete-ordinate method (FDDO) is a numerical method to simulate low density flow fields. In the FDDO method, the Boltzmann equation simplified by a model collision integral is transformed into a set of partial differential equations which are continuous in physical space. This is done by employing the discrete-ordinate method. The phase- space dependence of the model Boltzmann equation is effectively removed by replacing the integration over the phase-space of the distribution functions by appropriate quadrature formulas. The set of partial differential equations are then solved by means of a finite-difference approximation.

In the present study, two different approaches, the FDDO and the DSMC methods, are employed in the analysis of a rarefied gas flowing through a two-dimensional nozzle with a realistic nozzle lip and expanding into a surrounding vacuum environment. A computer code which was developed by Chung *et al.* [2,3] to investigate the flow of rarefied gases through internal geometries has been extended to simulate the flow around a more complex geometry. The feasibility of the FDDO method in analyzing this kind of flow is demonstrated by comparing the results with those of the DSMC method.

## 2. Problem Statement

Consider the steady flow of a single component, monatomic gas through a two dimensional nozzle, as shown in Fig. 1. The equilibrium number density, temperature, and pressure of the gas at the stagnation chamber upstream of the nozzle inlet are denoted as $n_o$, $T_o$ and $P_b$, respectively. The equilibrium number density, temperature, and pressure of the gas in the surrounding low-density environment are denoted as $bn_o$, $T_b$, and $P_b$ respectively. The temperature of the nozzle surface is denoted as $T_w$. The width of the nozzle inlet is $2Y_o$ and that of the exit is $2Y_e$. The nozzle has a constant width section of length $l_1$ and a diverging section of length $l_2$ with a diverging angle $\theta$. The width of the nozzle lip facing the downstream is $l_3$ and the length of the nozzle lip facing the positive $y$-direction is $l_4$.

## 3. Finite-Difference Method

### 3.1 Governing Equation

We consider the steady-state model Boltzmann equation without an external force in a Cartesian coordinate system, as illustrated in Fig. 1:

$$V_x \frac{\partial f}{\partial x} + V_y \frac{\partial f}{\partial y} = J_m \qquad (1)$$

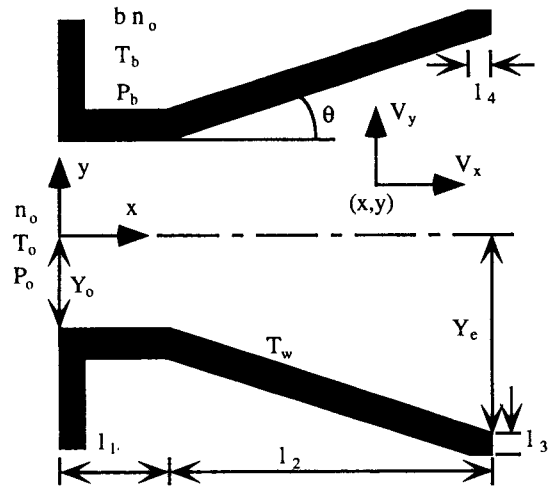


**Fig. 1** Nozzle Geometry

where $x$ and $y$ are Cartesian coordinates of the physical space, $V_x$ and $V_y$ are the velocity components of the molecules, $f(x, y, V_x, V_y)$ is the distribution function and $J_m$ is the model Boltzmann collision integral, which is some functional of $f$. The moments $n$, $U$, and $T$ are given by

$$n = \int f dV$$
$$nU = \int Vf dV \qquad (2)$$
$$3nRT = \int C^2 f dV$$

where $R$ is the gas constant and $C$ is the peculiar velocity, $V-U$.

The collision integral of the kinetic models, $J_m$, can be represented generally in a form

$$J_m = A_c(F-f) \qquad (3)$$

Here $A_cF$ approximates the replenishing collisions, and $A_cf$ the depleting collisions. The collision frequency, $A_c$, usually is a function of moments and is independent of molecular velocities, whereas $F$ is a function of both moments and molecular velocities.

In the present study the BGK model [4] is chosen for the sake of simplicity. In this model, $F$ is given by the Maxwell-Boltz mann distribution:

$$F = n(2\pi RT)^{-3/2} e^{(-C^2/2RT)} \qquad (4)$$

The collision frequency $A_c$ is taken to be of the form

$$A_c = \frac{mnRT}{\mu} \qquad (5)$$

where $m$ is the molecular mass. The viscosity $\mu$ is assumed to have a temperature dependency [5]

$$\frac{\mu}{\mu_o} = \left(\frac{T}{T_o}\right)^{\sigma} \qquad (6)$$

where $\sigma$ is a constant for a given gas. The viscosity at the stagnation chamber upstream of the inlet, $\mu_o$, is related to the mean free path $\lambda_o$ in the stagnation chamber by the relation

$$\lambda_o = \frac{16}{5} \frac{\mu_o}{mn_o(2\pi RT_o)^{1/2}} \qquad (7)$$

To reduce the number of independent variables, the following reduced distribution functions are introduced [6]:

$$g(x, y, V_x, V_y) = \int_{-\infty}^{+\infty} f(x, y, V_x, V_y) dV_z \qquad (8)$$

$$h(x, y, V_x, V_y) = \int_{-\infty}^{+\infty} V_z^2 f(x, y, V_x, V_y) dV_z \qquad (9)$$

By integrating out the $V_z$ dependence with the weighting functions 1 and $V_z^2$, respectively, the equations for the reduced distribution functions with the collision integral of kinetic models of Eq. (3) are obtained from Eq. (1):

$$V_x \frac{\partial g}{\partial x} + V_y \frac{\partial g}{\partial y} + A_c g = A_c G \qquad (10)$$

$$V_x \frac{\partial h}{\partial x} + V_y \frac{\partial h}{\partial y} + A_c h = A_c H \qquad (11)$$

where

$$G(x, y, V_x, V_y) = \int_{-\infty}^{+\infty} F dV_z$$

$$H(x, y, V_x, V_y) = \int_{-\infty}^{+\infty} V_z^2 F dV_z$$

By introducing a polar coordinate system for molecular velocity space which is defined as

$$V_x = V\sin\varphi$$
$$V_y = V\cos\varphi \qquad (12)$$
$$\varphi = \tan^{-1}(V_x/V_y)$$

and applying general transformation rules for physical space, the governing equations in the new coordinate system $(\eta, \xi)$ are written as [7]

$$B\frac{\partial g}{\partial \eta} + C\frac{\partial g}{\partial \xi} + A_c g = A_c G \qquad (13)$$

$$B\frac{\partial h}{\partial \eta} + C\frac{\partial h}{\partial \xi} + A_c h = A_c H \qquad (14)$$

where

$$B=(V\cos\varphi\, x_\xi - V\sin\varphi\, y_\xi)/J_t$$

$$C=(V\sin\varphi\, x_\eta - V\cos\varphi\, y_\eta)/J_t$$

and $J_t$ is the Jacobian of the transformation.

### 3.2 Discrete-Ordinate Method

In order to remove the velocity space dependency from the reduced distribution functions, the discrete-ordinate method [6] is employed. This method, which consists of replacing the integration over velocity space of the distribution functions by appropriate integration formulas, requires the values of the distribution functions only at certain discrete speeds and velocity angles. The choice of the discrete values of $V$ and $\varphi$ are dictated by the consideration that the final interest is not in the distribution functions themselves but in the moments. Hence, the macroscopic moments given by integrals over the molecular velocity space can be calculated by proper integration formulas. Applying the method, the following quadratures are substituted for the integrals in Eqs. (2):

$$n=\sum_\delta \int_0^{2\pi} P_\delta g_\delta\, d\varphi$$

$$nU_x=\sum_\delta \int_0^{2\pi} P_\delta V_\delta \sin\varphi\, g_\delta\, d\varphi$$

$$nU_y=\sum_\delta \int_0^{2\pi} P_\delta V_\delta \cos\varphi\, g_\delta\, d\varphi \qquad (15)$$

$$\frac{3}{2}nT=\sum_\delta \int_0^{2\pi} P_\delta (h_\delta + V_\delta^2 g_\delta)\, d\varphi - n(U_x^2+U_y^2)$$

$$(\delta = 1,2,3,\cdots,N-1,N)$$

where $P_\delta$ is the weights of the modified Gauss-Hermite quadrature [7,8] for the discrete speed $V_\delta$, and $g_\delta$ and $h_\delta$ denote $g(\xi,\eta,V_\delta,\varphi)$ and $h(\xi,\eta,V_\delta,\varphi)$, respectively. Thus, instead of solving the equations for a function of physical space and molecular velocity, the equations are transformed to partial differential equations which are continuous in physical space but are point functions in molecular speed V and velocity angle.

$$B\frac{\partial g_\delta}{\partial \eta} + C\frac{\partial g_\delta}{\partial \xi} + A_c g_\delta = A_c G_\delta \qquad (16)$$

$$B\frac{\partial h_\delta}{\partial \eta} + C\frac{\partial h_\delta}{\partial \xi} + A_c h_\delta = A_c H_\delta \qquad (17)$$

where

$$B=(V_\delta\cos\varphi\, x_\xi - V_\delta\sin\varphi\, y_\xi)/J_t$$

$$C=(V_\delta\sin\varphi\, x_\eta - V_\delta\cos\varphi\, y_\eta)/J_t$$

$$G_\delta=\frac{V_o^2}{n_o}\int_{-\infty}^{+\infty} f(\xi,\eta,V_\delta,\varphi,V_z)dV_z$$

$$H_\delta=\frac{1}{n_o}\int_{-\infty}^{+\infty} V_z^2 f(\xi,\eta,V_\delta,\varphi,V_z)dV_z$$

### 3.3 Numerical Procedure

The finite-difference approximations of Eqs. (16) and (17) are solved by the method of successive approximations. Details of the method may be found in Refs. 2, 3, and 7. In each iteration step, the calculation starts at the point $(\eta=\eta_\infty-\triangle\eta,\ \xi=\xi_\infty+\triangle\xi)$ for a chosen discrete-ordinate $V_\delta$. For this discrete-ordinate, the values of the distribution functions are then determined at all $(\eta,\xi)$ grid points for the quadrant of velocity angle $\pi/2\le\varphi\le\pi$. Then, applying the symmetric condition, the values of the distribution functions at the centerline are determined for the quadrant of velocity angle $\pi/2\ge\varphi\ge0$ and calculated at all $(\eta,\xi)$ grid points starting from the point $(\eta=\triangle\eta,\ \xi=\xi_{-\infty}+\triangle\xi)$. An analogous procedure is carried out for the quadrant of velocity angle $-\pi\le\varphi\le-\pi/2$ and $-\pi/2\le\varphi\le0$ starting from the point $(\eta=\eta_\infty-\triangle\eta,\ \xi=\xi_{-\infty}-\triangle\xi)$ and $(\eta=\triangle\eta,\ \xi=\xi_{-\infty}-\triangle\xi)$, respectively. After this procedure is repeated for all discrete-ordinates $V_\delta$ for both $g_\delta$ and $h_\delta$, the moments may

be calculated by means of the quadrature formula, Eqs. (15), with a proper integration method over the angle. The iterative procedure is stopped when the relative change in the density between two iterative steps is less than $10^{-3}$ for all spatial grid points. As a proper quadrature formula, the modified Gauss-Hermite half range quadrature for integrals of the form [7,8]

$$\int_0^\infty e^{-V^2} V^j Q(V) dV = \sum_{s=1}^{N} P_s Q(V_s) \qquad (18)$$

is used. The exponent $j$ and the order of the quadrature $N$ are chosen to be 1 and 16, respectively. Simpson's 3/8th rule with $\triangle\varphi = 4.5^o$ is used for the integration over the angle $\varphi$. The $(\eta, \xi)$ plane was covered by 101x51 grid points for the stagnation chamber upstream of the nozzle inlet, $50\times201$ for the region inside of the nozzle, $101\times51$ for the plume, and $51\times51$ for the backflow region. The exponent of the viscosity-temperature relation in Eq. (6), $\sigma$, was that for Argon, 0.811. The surface temperature was chosen to be the same as the stagnation chamber temperature, $T_o$.

## 4. Direct Simulation Monte-Carlo Method

In the present study, the no time count (NTC) method developed by Bird [9] is used as a sampling technique. In the NTC method, the number of pairs to be sampled, $N_s$, is given by

$$N_s = N_m n (\sigma_T C_r)_{\max} \triangle t/2 \qquad (19)$$

where $N_m$ is the number of simulated molecules in the cell, $\sigma_T$ is the collision cross-section, $C_r$ is the relative speed between colliding molecules, and $\triangle t$ is the discrete time interval. The collision probability for each selection is

$$\frac{(\sigma_T C_r)}{(\sigma_T C_r)_{\max}} \qquad (20)$$

For the calculation of molecular interaction, the variable hard sphere (VHS) model developed by Bird [10] is employed. In the VHS model, the collision cross-section is given by

$$\sigma_T \propto C_r^{-2\omega} \qquad (21)$$

where $\omega$ is related to the viscosity-temperature exponent, $s$, by

$$s = \omega + 0.5 \qquad (22)$$

In DSMC calculations, the best results are obtained when a large number of simulated molecules are used, when the cell size is as small in comparison with the mean free path, and when the discrete time step is as small in comparison with the mean collision time. In most of the calculations, the cell size, $\triangle x$ and $\triangle y$, was less than 1.0 and the time step was less than 0.25. Here the cell size is measured in units of the local mean free path and $\triangle t$ in units of the mean collision time based on the stagnation chamber condition.

The average number of molecules per cell was kept around 20 except for some cells in the backflow region where the normalized density decreases more than 5 orders of magnitude. Sampling interval was $5\triangle t$ and average sample size per cell was around 100,000. The exponent of the VHS model, $\omega$, was that for Argon, 0.311.

## 5. Results and Discussion

For the comparison of two methods the following geometric configurations are used in the calculations: $l_1 = 1$, $l_2 = 3$, $l_3 = 0.2$, $l_4 = 0.2$, and $\theta = +20^o$. The Knudsen number was chosen to be $K_n = 0.01$.

A comparison of the solutions inside the

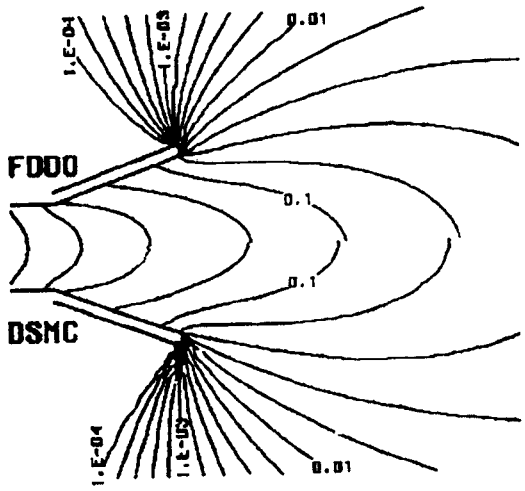


Fig. 2 Comparison of density contours, $n/n_o$.

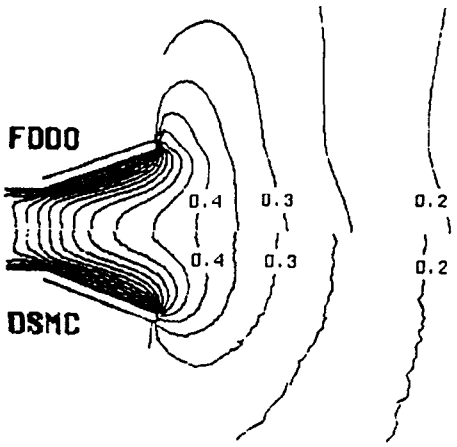


Fig. 3 Comparison of temperature contours, $T/T_o$.

nozzle, in the plume, and in the backflow region is made in Figs. 2 and 3, respectively, in which density and temperature contours are shown. The FDDO solutions are in the upper portion of the figures, and the DSMC solutions are in the lower portion. The density contours obtained by the two methods show good agreement in the entire flow domain. In some parts of the backflow region, however, a severe scattering of data appeared in the results of the DSMC method if the normalized density was lower than $10^{-4}$, which made it meaningless to compare the results. Hence, the density contours are plotted only up to $10^{-4}$. A logarithmic scale is used for the density contour. The temperature contours show good agreement inside the nozzle and near the exit plane. A severe scattering of data appeared in the temperature obtained by the DSMC method for a normalized density lower than $10^{-3}$, which is the entire portion of the backflow region. Hence, the temperature contours in the backflow region are not shown. A considerably greater computational effort will be required to resolve the scattering in the backflow region, which is beyond the scope of the present study.

In Fig. 4, density and temperature distributions are compared along the centerline of the nozzle. The density and temperature dis-

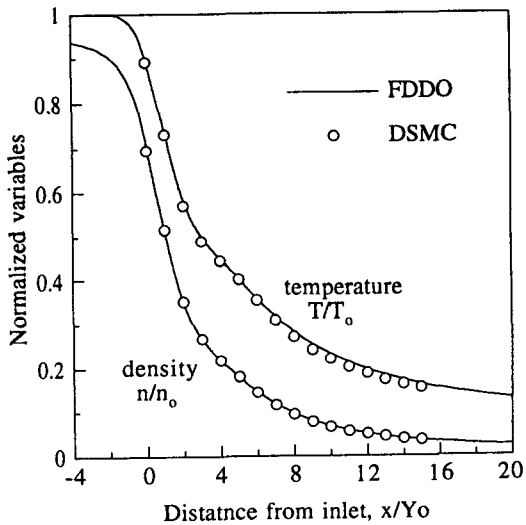


Fig. 4 Comparison of density and temperature distributions along the centerline of the nozzle.

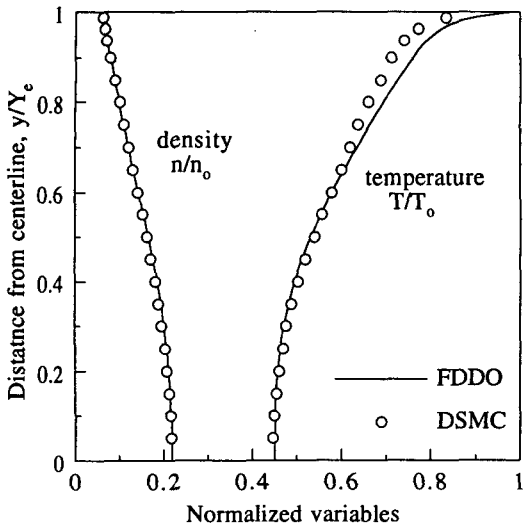


**Fig. 5** Comparison of density and temperature distributions at the exit plane of the nozzle.

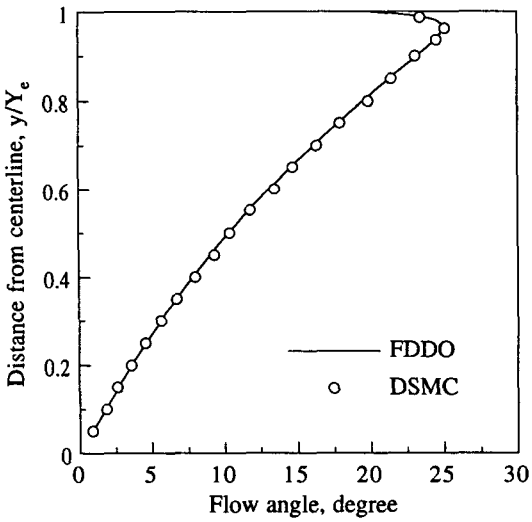


**Fig. 6** Comparison of flow angle at the exit plane of the nozzle.

tributions obtained by the two methods show very good agreement. In the plume, however, the temperature predicted by the FDDO method is slightly higher than that by the DSMC method. The FDDO method thus predicts a slightly slower expansion of the flow than does the DSMC method.

Figure 5 shows density and temperature distributions at the exit plane of the nozzle. The results from both methods show good agreement except for the temperature distribution near the wall where the DSMC method shows a slightly higher temperature than the FDDO method. In Fig. 6, the flow angle obtained by the two methods at the exit plane of the nozzle are compared. The maximum flow angle at the nozzle exit plane is about $25^o$, which exceeds the diverging angle of the nozzle wall $20^o$. It is interesting to note that the portion of the exit plane where the flow angle exceeds the divergence angle of the nozzle is about 20% of the exit-plane area and occurs near the wall. This portion of the flow significantly contributes to the back-scattering of the plume to the backflow region.

## 6. Conclusions

Two different approaches, the finite-dif ference method coupled with the discrete-ordinate method (FDDO), and the direct simulation Monte-Carlo (DSMC) method, were used in the analysis of the flow of a rarefied gas through a two-dimensional nozzle. The FDDO method has been shown to be a practical method for treating the flow of rarefied gases through a nozzle and expanding into a low-density background. The results of the FDDO and DSMC methods show good agreement for such flow variables as density, velocity, and temperature inside the nozzle and in the plume.

## References

[1] Bird, G. A., Molecular Gas Dynamics, Clarenden Press, Oxford (1994).

[2] Chung, C. H., De Witt, K. J., Jeng, D. R., and Keith, T. G. Jr., "Numerical Analysis of Rarefied Gas Flow Through Two-

Dimensional Nozzles," J. of Propulsion and Power, **11**-1 (1995), p.71.

[3] Chung, C. H., Jeng, D. R., De Witt, K. J., and Keith, T. G. Jr., "Numerical Analysis of Rarefied Gas Flow Through a Slit," J. Thermophysics and Heat Transfer, **6**-1 (1992), p.27.

[4] Bhatnagar, P. L., Gross, E. P., and Krook, M., "A Model for Collision Processes in Gases. I. Small Amplitude Processes in Charged and Neutral One-Component Systems," Phys. Rev., **94**-3 (1954), p. 511.

[5] Chapman, S., and Cowling, T. G., The Mathematical Theory of Non-Uniform Gases, Cambridge University Press, London (1958).

[6] Huang, A. B., "Georgia Institute of Technology, School of Aerospace Engineering Rarefied Gas Dynamics and Plasma Laboratory, Report No. 4 (1967).

[7] Chung, C. H., "Numerical Simulation of Rarefied Gas Flow Through Nozzles and Over Submerged Bodies," Ph.D. Thesis, University of Toledo (1990).

[8] Shizgal, B., "A Gaussian Quadrature Procedure for Use in the Solution of the Boltzmann Equation and Related Problems," J. of Computational Physics, **41** (1981), p.309.

[9] Bird, G. A., "The perception of Numerical Methods in Rarefied Gas Dynamics," Progress in Astronautics and Aeronautics: Rarefied Gas Dynamics, Muntz, E.P. et al (Ed.), AIAA, New York, Vol.118 (1989), p.211.

[10] Bird, G. A., "Monte Carlo Simulation in an Engineering Context," Progress in Astronautics and Aeronautics: Rarefied Gas Dynamics, Fisher, S.S. (Ed.), Vol. 74, AIAA, New York (1981), p.239.